CONCRETE LIBRARY OF JSCE NO. 27, JUNE 1996

SHEAR STRENGTH OF PRESTRESSED CONCRETE BEAMS WITH FRP TENDON

(Translation from Proceedings of JSCE. No.520/V-28, August 1995)

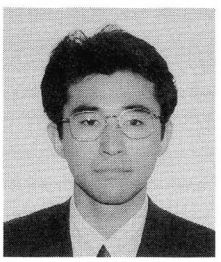

Yasuhiko SATO

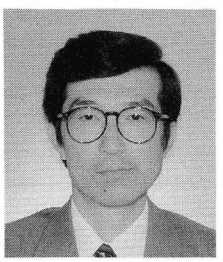

Tamon UEDA

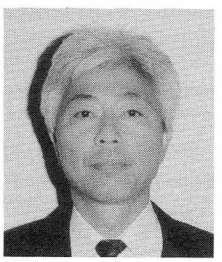

Yoshio KAKUTA

The shear resisting model for concrete beams reinforced with FRP rod proposed by the authors in a previous study is expanded to predict the shear strength of prestressed concrete beams with FRP tendon. The shear resisting model consists of four shear resisting forces which are defined as function of prestressing force, concrete strength, shear span to effective depth ratio, stiffness of tendon, and shear reinforcement. The applicability of the model is confirmed by comparing with experimental results.

Keywords : *FRP rods, PC beams, shear strength, shear reinforcement, non-linear finite element analysis*

Yasuhiko Sato is an assistant in the Department of Civil Engineering at Hokkaido University, Sapporo, Japan. He obtained his D.Eng. from Hokkaido University in 1994. His research interests relate to shear capacity of reinforced and prestressed concrete members. He is a member of JSCE.

Tamon Ueda is an Associate Professor in the Department of Civil Engineering at Hokkaido University. He obtained his D.Eng. from the University of Tokyo in 1982. His research interests relate to the deformation mechanism of concrete and composite structures. He is a member of JSCE.

Yoshio Kakuta is a Professor in the Department of Civil Engineering at Hokkaido University. He obtained his D.Eng. from Hokkaido University in 1968. His research interests include cracking, shear and fatigue of reinforced concrete members, partial prestressed concrete and application of continuous fiber reinforcing materials to concrete structures. He is a member of JSCE.

1. INTRODUCTION

It is desirable to promote the use of fiber reinforced plastic (FRP) rod as tendon for prestressed concrete (PC) members because of its favorable properties such as high strength and excellent anticorrosion resistance.

The main target of previous studies was to estimate the flexural behavior of prestressed concrete members using FRP tendon. As a result, it has been confirmed that flexural capacity can be predicted by the ordinary beam theory [1]. There is, however, no precise method for calculating shear capacity, although studies on shear behavior have been conducted. The reason is considered to be that the influence of mechanical characteristics of reinforcement as well as the effect of prestressing force have not been clarified.

An analytical investigation was conducted by the authors to show how shear resisting behavior of concrete beams differs in different mechanical properties of steel and/or FRP rod as reinforcement [2]. Based on the results, the shear strength equation for reinforced concrete beams with FRP rod as tension and/or shear reinforcement was developed [3]. This paper aims to quantitatively explain how prestressing force affects each shear resisting force component which appears in the shear strength equation for RC beams. Shear failure caused by fracture of FRP rod is, however, not considered in this study.

2. OUTLINE OF ANALYSIS

2.1 Finite Element Program

The non-linear finite element program used in this study was developed for shear problems of reinforced concrete beams [4] . A smeared crack model which adopts average stress and strain relationships is used in this program.

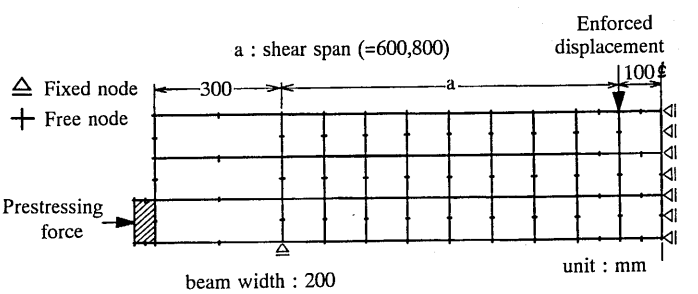

Fig.1 Finite Element Mesh

2.2 Analytical Method

Figure 1 shows the finite element mesh in this study. It is a simply supported rectangular cross section beam subjected to two-point monotonic loading. Because of symmetry, half of the beam was analyzed. Enforced displacements were given at the loading points and prestressing forces were applied as a load at a node of steel element attached to the specimen.

2.3 Analytical Parameters

It is generally known that there are many parameters which affect the shear strength of concrete beams. In this study, the following parameters, which are the prestressing force as the main parameter and others to develop the shear strength equation for concrete beams reinforced with FRP rod [4], are chosen (chosen values of the parameters in parentheses).
①prestressing force (P_{eff}=78～470kN)

②concrete strength (f_c' =29,44 and 59MPa)
③ratio of shear span to effective depth (a/d=2.4 and 3.2)
④stiffness of tendon (p_sE_S=2472 and 4944MPa)
⑤stiffness of shear reinforcement (p_wE_w=137,412 and 824MPa)
where:

p_s : tendon ratio
E_s : Young's modulus of tendon
p_w : shear reinforcement ratio
E_w : Young's modulus of shear reinforcement

The average prestresses in concrete were selected to be 4.5%, 9%, and 13.5% of concrete strength, while the maximum prestresses in a section ranged between about 10% and 35%. Beam width and height were fixed at 200 mm and 300 mm, respectively. The target in this study was to develop a shear strength equation for PC beams using FRP rod as tendon and/or shear reinforcement. Influences of tendon and shear reinforcement on the shear strength are estimated from stiffness [3]. Analytical specimens contain only tendon as tension reinforcement.

Generally, shear strength differs for different positions of prestressing force [5]. In this study, the position of prestressing force was fixed in such a way that extreme tension fiber strains were compression. Experimental and analytical results show that the size of loading plates affects shear strength of beams whose shear span to effective depth ratio is rather small [6]. However, this effect is not taken into account in this study. Neither is the effect of compressive reinforcement considered.

2.4 Failure Mode in Analysis

In the analyses, softening of concrete around the loading point was observed at peak load. It can be said that the failure mode is shear compression failure. Therefore, the shear strength equation developed in this study by numerical experiment can be applied to concrete beams in which shear compression failure occurs.

3. SHEAR RESISTING MODEL OF CONCRETE BEAMS REINFORCED WITH FRP RODS

3.1 Shear Resisting Model

The shear resisting model developed by the authors is defined by the following equation as the summation of shear forces sustained by various resisting components (see Fig.2).

$$V = V_{cpz} + V_{web} + V_{str} - V_{com} \tag{1}$$

where

V_{cpz} : shear force carried by concrete in compression zone above a neutral axis
V_{str} : shear force carried by other than shear reinforcement in shear cracking zone
V_{web} : shear force carried by shear reinforcement in shear cracking zone
V_{com} : shear force transferred by concrete in horizontal zone

In Eq.(1), the horizontal zone is defined to connect the failure section in compression zone near the loading point with the shear cracking path where shear force carried is the largest.

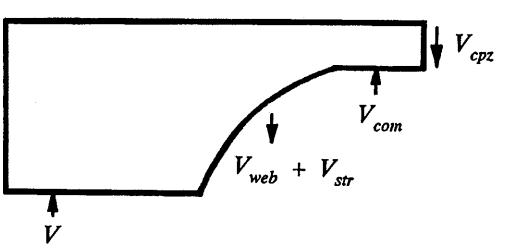

Fig.2 Shear Resisting Model

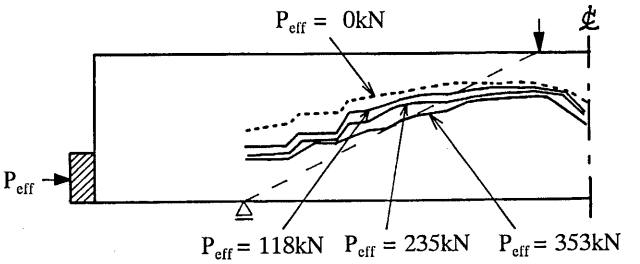

Fig.3 Location of Neutral Axis in Analytical Specimen

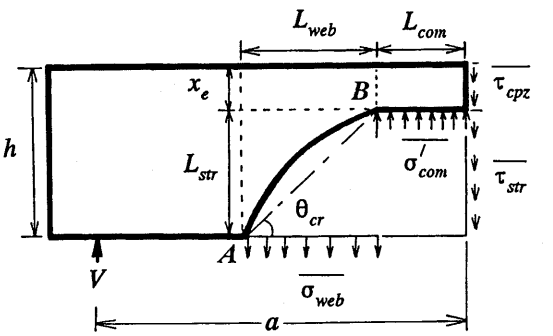

Fig.4 Distribution of Shear Resisting Stresses

Figure 3 shows neutral axis lines in reinforced concrete beam specimens in which the shear span to effective depth ratio is 2.4. It is clearly observed that the depths to the neutral axis increase along with prestressing forces. If a point where the neutral axis line intersects with a straight line connecting the loading and supporting points is defined as an intersecting point, depth to the neutral axis is constant between loading point and intersecting point in the case of concrete beams without prestressing force [3]. In Fig.3, when P_{eff} is 353 kN, there is a part in which the depth is not constant. It can be said, however, that the depth is generally constant between loading and intersecting points. It is observed that the shear force at a shear cracking path through the intersecting point is the largest. Therefore the shear resisting model described in Eq.(1) is also used for prestressed concrete beams.

The shear force carried by each component is calculated by multiplying the stresses at gauss points (points of numerical integration for computation of stress and load vectors) along the cut plane shown in Fig.2 by the area which the respective gauss point covers. The shear force carried by compression zone is calculated using shear stress of concrete at the gauss point in the nearest section from the loading point (a distance of 11.3 mm from loading point). The shear force transferred at horizontal zone is calculated using concrete compressive stress. The shear force by shear reinforcement at shear cracking zone is calculated using tensile stress, which is a summation of average stress of the shear reinforcement and average stresses of concrete. The shear force carried by other than shear reinforcement at shear cracking zone is calculated using shear stress transferred by aggregate interlocking [2][3]. These shear forces are calculated by an integration of resisting stresses over the resisting zone. Equation (1) can be rewritten using average stresses at each resisting zone as follows.

$$V = bx_e\overline{\tau_{cpz}} + p_w L_{web}\overline{\sigma_{web}} + bL_{str}\overline{\tau_{str}} - bL_{com}\overline{\sigma'_{com}} \qquad (2)$$

where

$\overline{\tau_{cpz}}$: average shear stress at compression zone

$\overline{\sigma_{web}}$: average tensile stress of shear reinforcement at shear cracking zone

$\overline{\tau_{str}}$: average shear stress at shear cracking zone

$\overline{\sigma'_{com}}$: average compressive stress at horizontal zone

L_{web} : horizontal projected length of shear cracking zone
L_{str} : vertical projected length of shear cracking zone
L_{com} : length of horizontal zone
b : beam width
x_e : depth of compression zone

The length of horizontal zone is assumed as follows [3].

$$L_{com} = \frac{a}{h} x_e \qquad (a>h) \tag{3}$$

The angle of a line connecting a start point (A in Fig.4) with an end point (B in Fig.4) of shear crack in RC beams was assumed to be at 45° to the member axis [3]. This assumption means the angle of shear crack is almost identical for different stiffnesses of tension and shear reinforcement, etc.

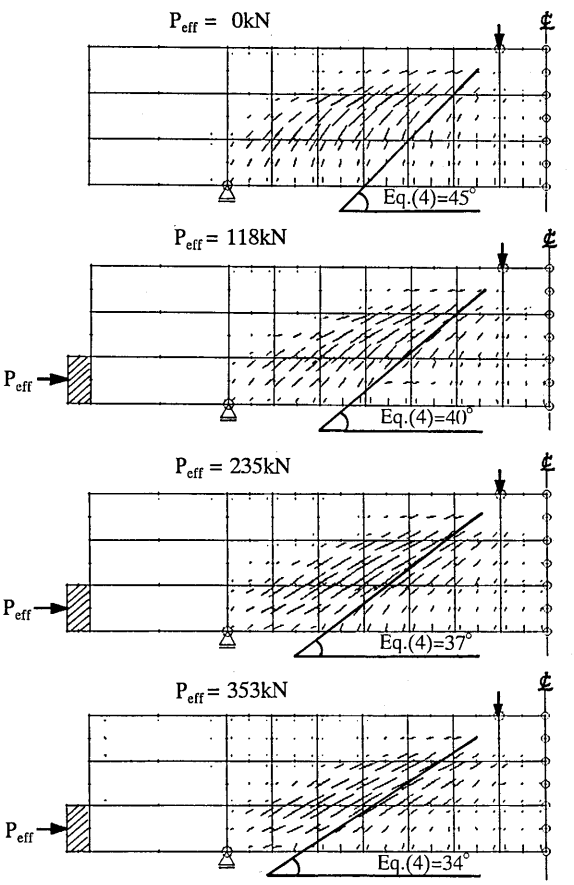

Fig.5 Crack Pattern of Analytical Specimens.

Figure 5 shows crack patterns of analytical specimens subjected to different prestressing forces. The angle of shear cracks gradually decreases as prestressing force increases. Therefore the angle θ_{cr} is calculated by the following equation.

$$\theta_{cr} = 45\,[1 - (\frac{\sigma_P'}{f_c'})^{0.7}] \qquad (deg) \tag{4}$$

where σ_P' is the prestressing force divided by the cross sectional area of the beam.

In the analytical specimens shown in Fig.5, the assumed angles of shear crack are 42° , 37° , and 34° and angles predicted by Eq.(4) are 40° , 37° , and 34° , respectively.

The horizontal projected length of shear cracking zone is defined as follows.

$$L_{web} = \frac{L_{str}}{\tan\theta_{cr}} \tag{5}$$

where

$$L_{str} = h - x_e \tag{6}$$

The proposed model can be applied to a case in which the following geometric condition is satisfied.

$$L_{com} + L_{web} < a \tag{7}$$

When the size of compression zone of failure section, x_e and the angle of shear crack, θ_{cr} are given, the corresponding distribution area of each average stress can be calculated. The numerical experiment in this study investigates how analytical parameters shown in 2.3 affect the resisting area and stresses.

3.2 Size of Compression Zone

Figure 6 shows relationships between the size of compression zone and prestress. The size of compression zone at ultimate increases as prestress increases. It is observed also that the size of compression zone is greater when *a/d* is larger as in the case of RC beams [3] .

The size of compression zone in RC beams can be predicted by considering the depth calculated with the elastic theory in which tension in concrete is neglected [3]. This means that compression zone in pure-flexure region is almost the same as the value calculated by the elastic theory, and that compression zone in flexure-shear region is less than the value calculated by the elastic theory.

Figure 7 shows relationships between prestress and the ratio of the depth of compression zone in flexural-shear region, x_e to that in pure-flexure region. The ratio is approximately the same for different prestressing forces. It is therefore considered that, based on the depth in pure-flexure region, the depth at failure section in flexural-shear region can also be defined for prestressed concrete beams. However, the depth to neutral axis predicted by the elastic theory in prestressed concrete beams is expressed by the function of compressive strain at extreme fiber in compression zone. For simplicity, therefore, the size of compression zone in PC beams is investigated by comparing with the value calculated by the elastic theory for RC beams as given in the following equation.

$$x = kd \tag{8}$$

$$k = -np_s + \sqrt{(np_s)^2 + 2np_s} \tag{9}$$

Figure 8 shows relationships between the size of the compression zone, x_e normalized by the depth predicted by Eq.(8), x and prestress normalized by concrete strength (hereafter called prestress level). From Fig.8(a) influence of concrete strength can be considered as prestress level. Therefore it is proposed that the size of compression zone in PC beams can be calculated by the following equation which is the equation for RC beams [3], modified by adding a new term for prestressing force.

$$\frac{x_e}{x} = \left(\frac{x_e}{x}\right)_{\sigma_P'=0} [1+(\frac{\sigma_P'}{f_c'})^{0.7}]$$

$$= \frac{1-e^{-(\frac{a}{d})}}{1+3.2^{-0.12(p_w E_w)^{0.4}}} [1+(\frac{\sigma_P'}{f_c'})^{0.7}] \quad (10)$$

Solid lines indicate the results predicted by Eq.(10). It is clearly seen that Eq.(10) can predict the results of the numerical experiment with reasonable accuracy.

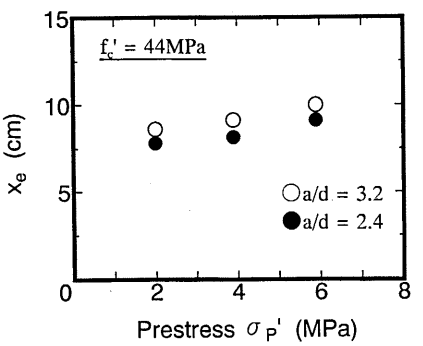

Fig.6 Relationship between Size of Compression Zone and Prestress

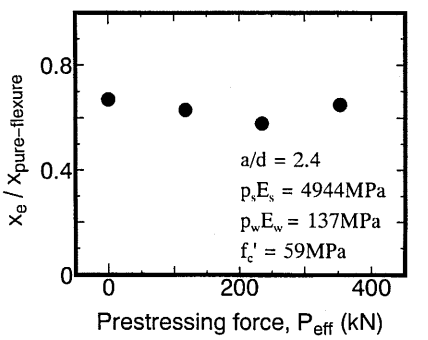

Fig.7 Relationship between Ratio of Compression Zone of Size in Flexure - Shear Region to that of Pure-Flexure Region and Prestressing Force

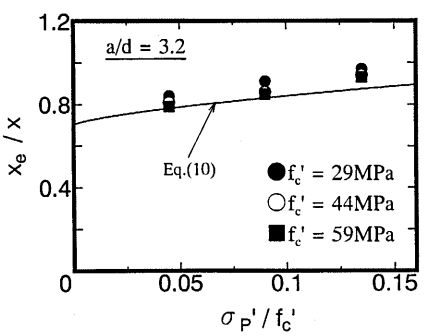

(a) For different concrete strengths

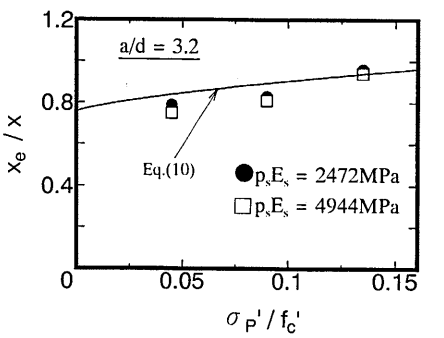

(b) For different tendon stiffnesses

Fig.8 Relationship between Normalized Size of Compression Zone and Prestress Level

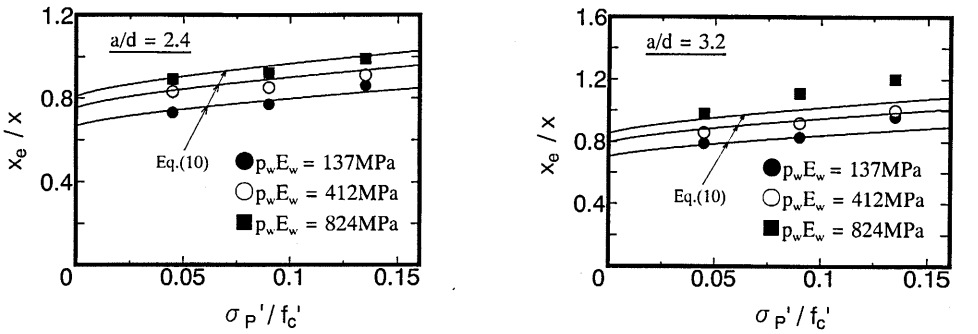

(c) For different shear reinforcement stiffnesses

Fig.8 Relationship between Normalized Size of Compression Zone and Prestress Level

3.3 Average Shear Stress at Compression Zone

To develop the failure criteria and equation for prediction of the average shear stress in compression zone, the principal stresses (see Fig.9) in compression zone are investigated.

Figure 10 shows relationships between prestress level and averages of maximum ($\overline{\sigma'_{1ave}}$) and minimum ($\overline{\sigma'_{2ave}}$) principal stresses. There is no influence of concrete strength, *a/d* and prestress level for average stresses, as in the case of RC beams [3]. It can be said that minimum and maximum principal stresses are 80% and 15% of uniaxial compressive strength, respectively. Furthermore, it is observed that these stresses are not influenced by stiffnesses of tendon nor shear reinforcement.

In this study, therefore, the same failure criteria as in the case of RC beams are assumed for the case of PC beams.

$$\frac{\overline{\sigma'_{2u}}}{f'_c} = 0.80 \tag{11}$$

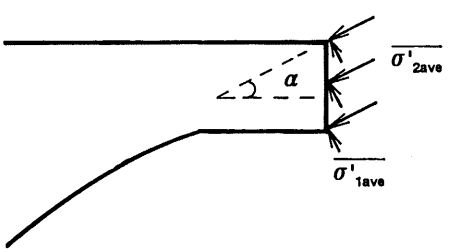

Fig.9 Principal Stress State in Compression Zone

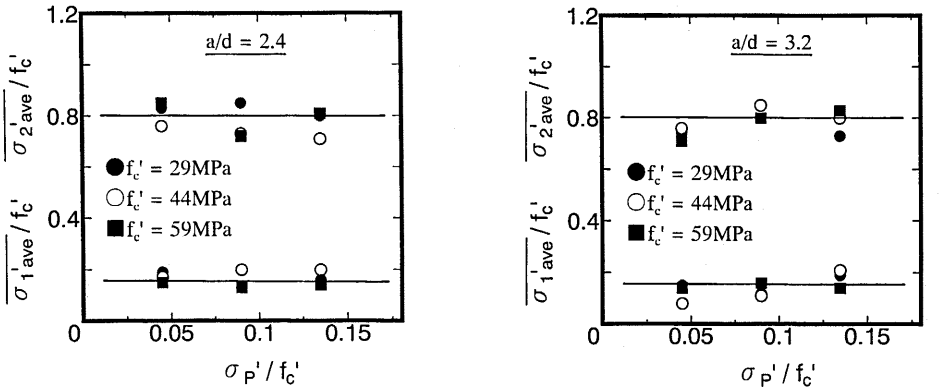

(a) For different concrete strengths

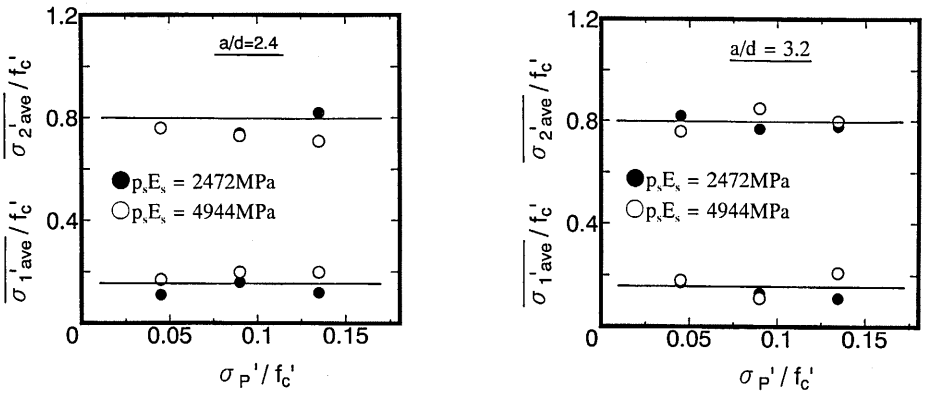

(b) For different tendon stiffnesses

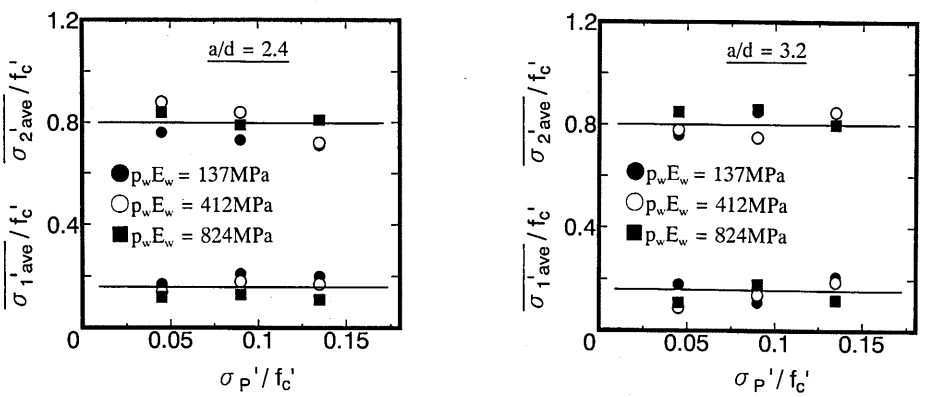

(c) For different shear reinforcement stiffnesses

Fig.10 Relationship between Average Principal Stress and Prestress Level

$$\frac{\overline{\sigma'_{1u}}}{f'_c}=0.15 \tag{12}$$

where $\overline{\sigma'_{2u}}$ and $\overline{\sigma'_{1u}}$ are, respectively, the average of minimum and maximum principal stress at failure.

On the other hand, Fig.11 shows relationships between angle of principal stress and prestress level. The angle in compression zone is approximately the same for different prestress levels and only the influence of *a/d* ratio is observed. Solid lines in Fig.11 show the value calculated by Eq.(13) which is the equation for angle of principal stress in RC beams. It is clearly seen that the equation is applicable to the case of PC beams.

$$\tan\alpha=\left(\frac{a}{d}\right)^{-1} \tag{13}$$

Finally, the average shear stress at compression zone $\overline{\tau_{cpz}}$ can be predicted by the following equation which is derived from Eqs.(11) and (12).

$$\frac{\overline{\tau_{cpz}}}{f'_c}=0.65\sin\alpha\cos\alpha \tag{14}$$

Figure 12 shows relationships between average shear stress and prestress level. The prediction by Eq.(14) agrees well with the analytical results. In this equation, $\overline{\tau_{cpz}}$ decreases as *a/d* increases in the range less than *a/d* of 1.0. Since this range does not satisfy the condition of Eq.(7), investigation for this range is not conducted in this study.

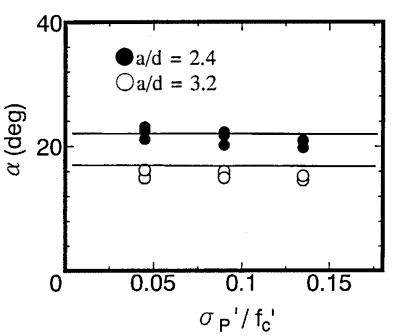

Fig.11 Relationship between Angle of Principal Stress and Prestress Level

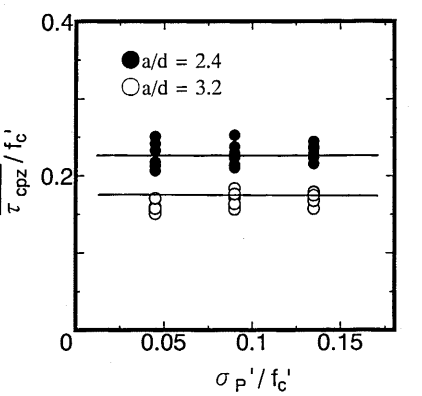

Fig.12 Relationship between Average Shear Stress at Compression Zone and Prestress Level

3.4 Average Compressive Stress at Horizontal Zone

Figure 13 shows principal stress state of concrete at horizontal zone. In all the specimens, average of maximum principal stress ($\overline{\sigma'_{1ave}}$) is less than 10% that of minimum principal stress ($\overline{\sigma'_{2ave}}$), so that the stress state can be assumed as an uniaxial stress state in which the minimum principal stress acts only as in the case of RC beams [3].

Figure 14 shows relationships between average minimum principal stress and prestress level. The stress increases proportionally to concrete strength. It can be said that the average stress is constant for different *a/d* ratios but there is no influence of stiffnesses of tendon and shear reinforcement. A solid line shows the stress predicted by Eq.(15) which is the equation for RC beams [3]. It can be said that the equation can evaluate the average stress for PC beams.

$$\frac{\overline{\sigma'_{2ave}}}{f'_c} = 0.64\left(\frac{a}{d}\right)^{-1} \tag{15}$$

On the other hand, Fig.15 shows relationships between the angle of principal stress and prestress level. The angle decreases as prestress level increases, and does not depend on other analytical parameters. In this study, therefore, the angle of principal stress at horizontal zone is given as a function of prestress level by the following equation.

$$\beta = (\beta)_{\sigma'_P=0}\left[1-\left(\frac{\sigma'_P}{f'_c}\right)^{0.5}\right]$$

$$= 32\left[1-\left(\frac{\sigma'_P}{f'_c}\right)^{0.5}\right] \quad (deg) \tag{16}$$

The solid line in Fig.16 show the values calculated by Eq.(16) which differs from the case of RC beams where the angle can be assumed to be a constant 32° [3]. Equation (16) indicates the angle decrease with increasing prestress level.

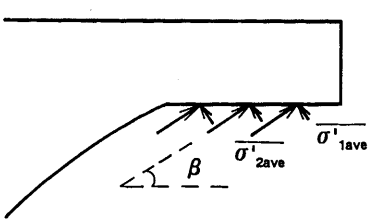

Fig.13 Principal Stress State in Horizontal Zone

Finally, the average normal stress (normal component of $\overline{\sigma'_{2ave}}$), which is compressive stress, can be calculated by the average principal stress given by Eq.(15) considering its angle predicted by Eq.(16).

$$\frac{\overline{\sigma'_{com}}}{f'_c} = 0.64\left(\frac{a}{d}\right)^{-1}\sin^2\beta \tag{17}$$

where $\overline{\sigma'_{com}}$ is the average compressive stress at horizontal zone.

Figure 16 shows relationships between the average compressive stress and prestress level. Solid lines show the values predicted by Eq.(17). It can be said that Eq.(17) can predict the tendency that the average compressive stress decrease as prestress level increases.

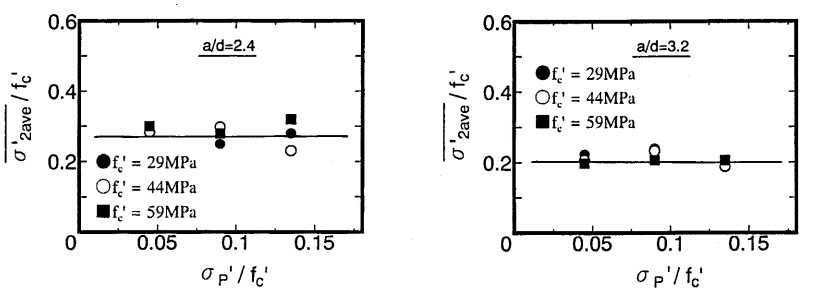

(a) For different concrete strengths

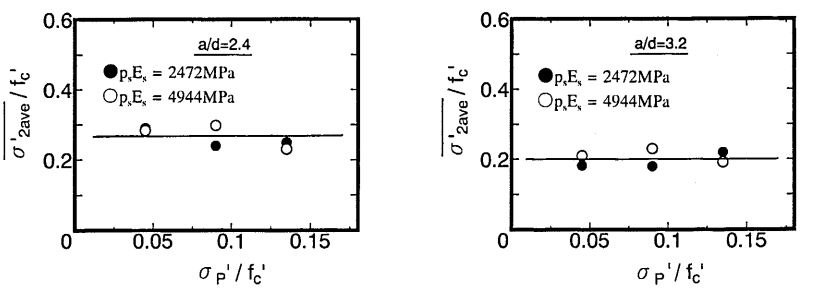

(b) For different tendon stiffnesses

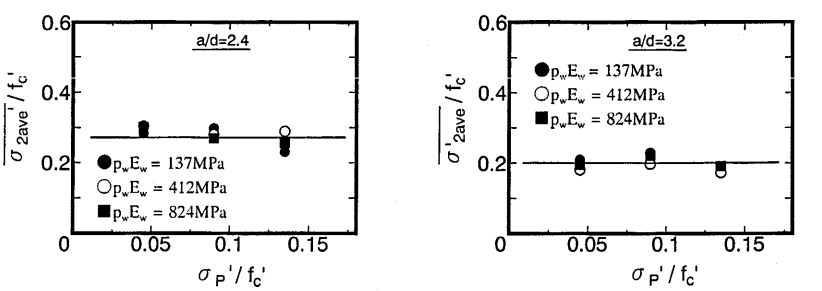

(c) For different shear reinforcement stiffnesses

Fig.14 Relationship between Average Principal Stress and Prestress Level

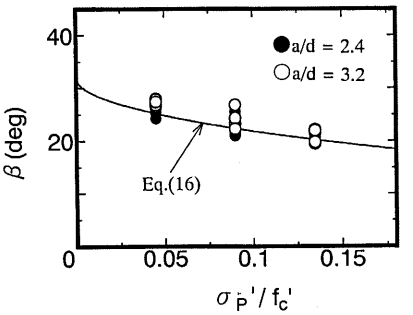

Fig.15 Relationship between Angle of Principal Stress and Prestress Level

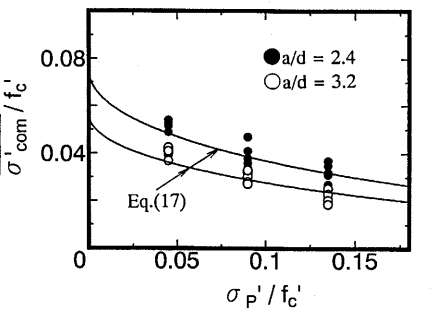

Fig.16 Relationship between Average Compressive Stress and Prestress Level

3.5 Average Shear Stress at Shear Cracking Zone

In the authors' previous study on shear resisting behavior of PC beams, shear resisting force carried by other than shear reinforcement at shear cracking zone decreases when prestressing force is applied. This is because stresses transferred by aggregate interlocking are lessened due to reduced shear deformation at shear cracks whose angles are reduced by prestressing [7].

Figure 17 shows relationships between average shear stress and prestress level. The shear stress decreases as prestress increases. The stress becomes greater when *a/d* is smaller as in the case of RC beams [3].

The effect of prestress is investigated based on the average shear stress in RC beams. Figure 18 shows relationships between average shear stress divided by shear stress in the case of no prestress and prestress level. From Fig.18(a), the shear stress decreases with increasing prestress level in a similar fashion for different concrete strengths, which is also found in the case of RC beams [3]. It can be said that for the same prestress level the average shear stress is approximately the same for different stiffnesses of main and shear reinforcement.

In this study, therefore, it is assumed that the average shear stress predicted by the equation for RC beams decreases with an increase in prestress level as follows.

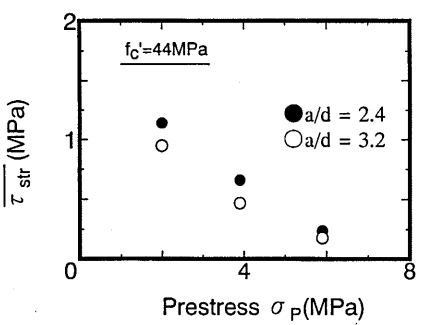

Fig.17 Relationship between Average Shear Stress at Shear Cracking Zone and Prestress

$$\frac{\overline{\tau_{str}}}{f_c'^{1/3}} = \left(\frac{\overline{\tau_{str}}}{f_c'^{1/3}}\right)_{\sigma_P'=0} \cdot e^{-11.2\frac{\sigma_P'}{f_c'}}$$

$$= \frac{1.28}{\sqrt{a/d}+1} e^{-11.2\frac{\sigma_P'}{f_c'}} \tag{18}$$

It is indicated in Fig.18 that the solid lines obtained from Eq.(18) agree well with the results of the numerical experiment.

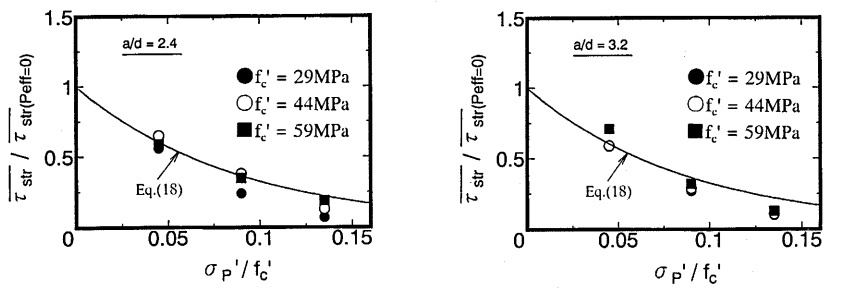

(a) For different concrete strengths

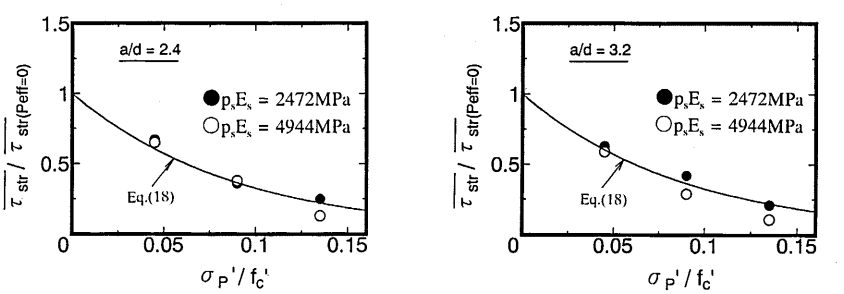

(b) For different tendon stiffnesses

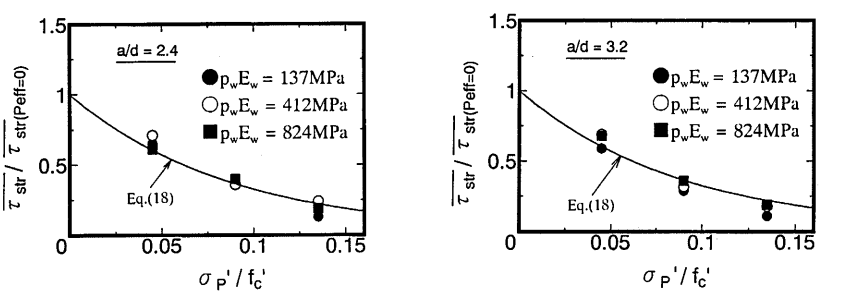

(c) For different shear reinforcement stiffnesses

Fig.18 Relationship between Average Shear Stress and Prestress Level

3.6 Average Tensile Strain on Shear Reinforcement at Shear Cracking Zone

The equation for prediction of the shear force by shear reinforcement is developed by using average tensile strain of shear reinforcement as in the equation for RC beam [3].

Figure 19 shows relationships between average strain of shear reinforcement and prestress level. The strain at ultimate slightly increases as prestress level increases. Generally, the strain for the same applied shear force decreases as prestressing force increases [8]. In this numerical experiment the same phenomena is observed. However, the strain at ultimate becomes larger as prestressing force increases because shear strength of beam grows larger as prestressing force increases.

The average strain of shear reinforcement in the case of PC beams is investigated by comparing the average strain in the case of RC beams.

Figure 20 shows the relationships between tensile strain divided by tensile strain in RC beams and prestress level. For different concrete strengths, the average strain increases at the same rate as prestress level increases. In Figs. 20(b) and (c) , the rate of increase is the same for different stiffnesses of tendon and shear reinforcement.

In this study, therefore, the tensile strain is defined by the following equation derived from the equation for RC beams.

$$\overline{\varepsilon_{web}} = (\overline{\varepsilon_{web}})_{\sigma_P'=0} \cdot \left[1+\left(\frac{\sigma_P'}{f_c'}\right)^{0.2}\right]$$

$$= 0.0053 \frac{\sqrt{f_c'}}{\sqrt{a/d}+1} e^{\left(-\frac{1000}{p_s E_s}-0.05\sqrt{p_w E_w}\right)} \left[1+\left(\frac{\sigma_P'}{f_c'}\right)^{0.2}\right] \quad (19)$$

The solid lines in each figure which show the value predicted by Eq.(19) indicate that Eq.(19) can approximately evaluate the results of numerical experiment. As in the case of RC beams, *a/d*, concrete strength, stiffness of tendon and shear reinforcement affect the tensile strain of shear reinforcement at the shear cracking zone. The rate of increase in the shear reinforcement strain with increase in the magnitude of prestress can be considered uniquely by Eq.(19).

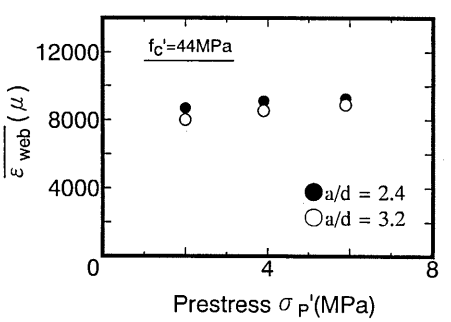

Fig.19 Relationship between Average Stirrup Strain and Prestress

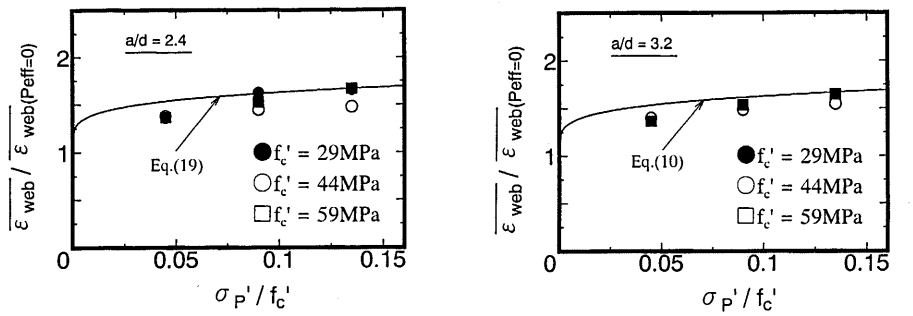

(a) For different concrete strengths

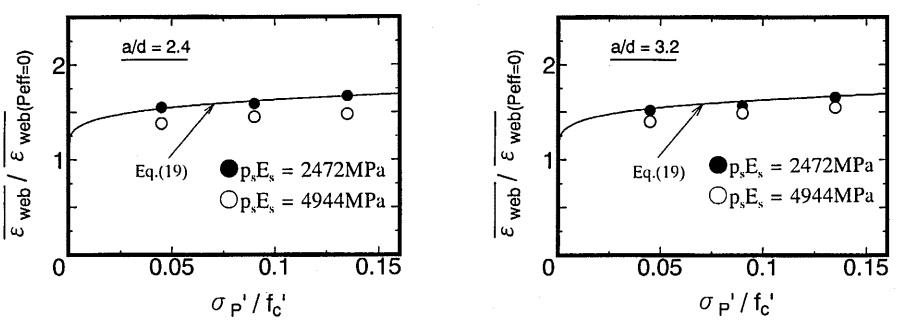

(b) For different tendon stiffnesses

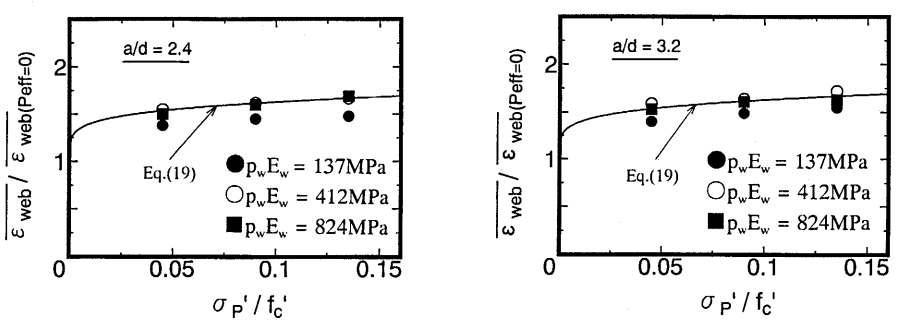

(c) For different shear reinforcement stiffnesses

Fig.20 Relationship between Average Stirrup Strain and Prestress Level

4. EVALUATION OF PROPOSED SHEAR STRENGTH EQUATION

4.1 Relationships between Shear Strength Equation and Influential Factors

The effects of concrete strength, shear span to effective depth ratio, stiffness of tendon and shear reinforcement, and prestressing force to the shear strength calculated by the equation proposed in Chapter 3 are investigated.

(1) Effect of concrete strength

Figure 21 shows the relationship between concrete strength and shear strength. In this case, the shear strength is normalized by the shear strength for the case where the concrete strength is 40 MPa while the stiffness of tendon and shear reinforcement, and *a/d* ratio are kept constant. The shear strength in concrete strength of 60 MPa is about 1.5 times of that of 20MPa. It can be said that concrete strength greatly affects the shear strength.

(2) Effect of shear span to effective depth ratio

Figure 22 shows the relationship between *a/d* and shear strength. The shear strength is normalized by the shear strength for the case where *a/d* is 3.0. The shear strength increases as *a/d* decreases. The ratio of shear force at shear cracking zone (V_{web}+V_{str}) to total shear force becomes greater as *a/d* decreases.

(3) Effect of tendon stiffness

Figure 23 shows the relationship between tendon stiffness and shear strength. The shear strength is normalized by the shear strength in the case that tendon stiffness is 4000 MPa. The shear strength increases as tendon stiffness increases, but the rate of increase is slow. At shear cracking zone, it is observed that the rate of shear force to total shear force gradually decreases as stiffness of tendon increases.

(4) Effect of stiffness of shear reinforcement

Figure 24 shows the relationship between stiffness of shear reinforcement and shear strength. The shear strength is normalized by the shear strength in the case where the stiffness of shear reinforcement is 400MPa. The shear strength increases as stiffness of shear reinforcement increases. The increase of shear strength depends on the increase of the shear force carried by shear reinforcement.

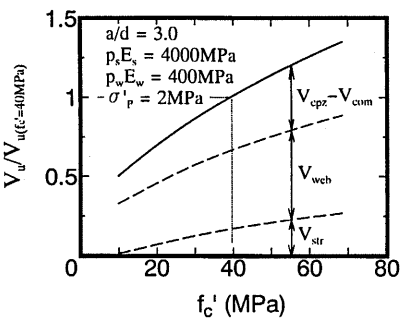

Fig.21 Relationship between Shear Strength and Concrete Strength

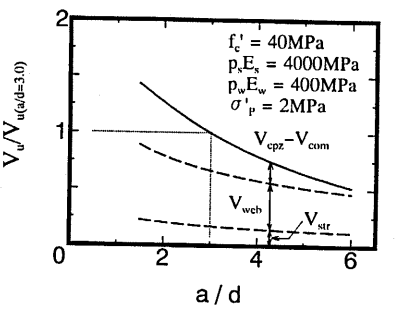

Fig.22 Relationship between Shear Strength and *a/d*

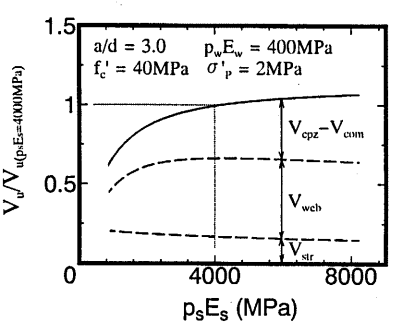

Fig.23 Relationship between Shear Strength and Stiffness of Tendon

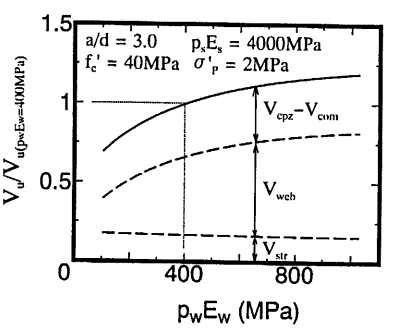

Fig.24 Relationship between Shear Strength and Stiffness of Shear Reinforcement

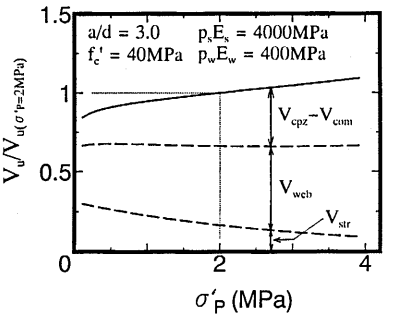

Fig.25 Relationship between Shear Strength and Prestress

(5) Effect of prestressing force

Figure 25 shows the relationship between prestress and shear strength. The shear strength is normalized by the shear strength in the case that prestress is 2 MPa. The shear strength increases as prestress increases. It is observed that the rate of shear resisting force at shear cracking zone ($V_{web}+V_{str}$) increases and the rate of other shear force ($V_{cpz}-V_{com}$) to total shear resisting force decreases as prestress increases. The decrease in the rate of shear resisting force at shear cracking zone is caused by the decrease of shear resisting force carried by other than shear reinforcement at shear cracking zone V_{str} as prestress increases.

4.2 Evaluation of Proposed Shear Strength Equation by Previous Experimental Results

The predicted results are compared with previous experimental results to confirm the applicability of the proposed model for prestressed concrete beams with FRP tendon.

In this study, experimental data from thirteen PC beams with rectangular cross section [9] are used. The outline of the beams are shown in Table 1. The *a/d* ratio is 3.0 for all specimens. In this table, V_{test} indicates the experimental shear strength, V_{cal} indicates the predicted shear strength, and A, C, and G indicate aramid, carbon, and glass fibers respectively.

Figure 26 shows the relationship between the predicted shear strength divided by experimental shear strength and the stiffness of shear reinforcement. It is observed that the predictions underestimate the experimental shear strengths. The average shear strength ratio is 1.18. It can be said that the scatter

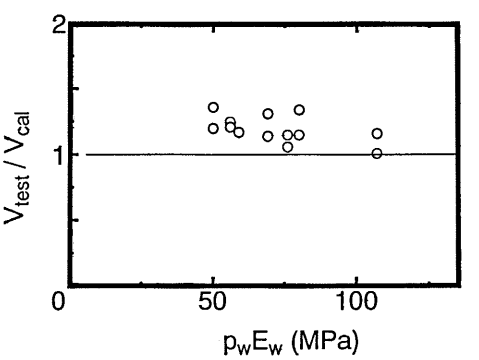

Fig.26 Relationship between Ratio of Shear Strength and Stiffness of Shear Reinforcement

is small since the coefficient of variation is 7.8%. Further study to compare predicted shear strength with various experimental results should be conducted in order to explain the discrepancy.

For concrete beams reinforced with FRP rods with a low stiffness of shear reinforcement (less than 100 MPa approximately), the proposed model overestimates its shear strength [3]. In beams which have a low stiffness of main and/or shear reinforcement, as well as beams without shear reinforcement, diagonal tension failure is caused by single cracking. The finite element program used in this study cannot exactly simulate the diagonal tension failure. Therefore the proposed model developed by the numerical experiment using this program cannot be applied to the diagonal tension strength.

In the case of PC beams, however, the proposed mode can predict the shear strength of beams with stiffness of shear reinforcement less than 100MPa.

From the experimental specimens, it was observed that the failure mode changes from diagonal tension failure to shear compression failure as the prestressing force increases [9]. Therefore the finite element program can evaluate the shear strength even when a beam has low shear reinforcement stiffness. It can be said, therefore, that the proposed model for prestressed concrete beams with FRP tendon developed by the numerical study can predict shear strength.

Table 1 Test Specimens and Shear Strengths [9]

Specimen	P_{eff} (kN)	f_c' (MPa)	Tendon			Shear reinforcement			V_{test} (kN)	V_{cal} (kN)	$\frac{V_{test}}{V_{cal}}$
			Type	p_s (%)	p_sE_s (MPa)	Type	p_w (%)	p_wE_w (MPa)			
C-G2-1	123	39	C	0.70	982	G	0.15	56	162	130	1.25
C-G1-1	125	39	C	0.70	982	G	0.21	80	157	137	1.15
C-G2-2	178	51	C	0.70	982	G	0.15	56	181	149	1.21
C-G1-2	179	47	C	0.70	982	G	0.21	80	199	149	1.34
C-A2-1	125	48	C	0.70	982	A	0.07	50	151	126	1.20
C-A1-1	125	38	C	0.70	982	A	0.10	69	170	130	1.31
C-A2-2	176	46	C	0.70	982	A	0.07	50	185	136	1.36
C-A1-2	177	60	C	0.70	982	A	0.10	69	200	175	1.14
C-C2-1	126	45	C	0.70	982	C	0.07	76	157	148	1.06
C-C1-1	126	41	C	0.70	982	C	0.10	107	152	151	1.01
C-C2-2	178	52	C	0.70	982	C	0.07	76	182	159	1.15
C-C1-2	177	51	C	0.70	982	C	0.10	107	194	168	1.16
C-CS2-2	175	52	C	0.70	982	C	0.04	59	178	152	1.17

5. CONCLUSION

In this study the following conclusions are obtained.

(1)Shear strength equation for prestressed concrete beams with FRP tendon is developed by numerical experiment using non-linear finite element analysis. The proposed shear strength equation is applicable for beams with shear compression failure. The failure criteria in the equation is defined by the principal concrete stress in compression zone. The shear force calculated by the proposed model is defined as a summation of shear resisting forces carried by concrete in compression zone, by shear reinforcement and others in shear cracking zone, and by concrete in horizontal zone linking the compression zone and shear cracking zone. These shear forces are calculated by multiplying each resisting zone by average stresses which are the function of prestress level, shear span to effective depth ratio, concrete strength, and stiffness of tendon and shear reinforcement.

(2) Shear strength predicted by the proposed model increases as concrete strength and/or shear span to effective depth ratio become larger. The shear strength gradually increases as tendon and shear

reinforcement stiffness and prestressing force increase.

(3) The applicability of the proposed model is confirmed by comparing with the experimental results. Comparison with various kinds of experimental results should be conducted since stiffness of tendon and shear span to effective depth ratio in beams used in this study is constant.

This study aims at the case in which eccentric prestressing force acts in the beams. Future study on the effect of position of prestressing force and partially prestressed concrete (PRC) member should be conducted to develop unified design equations. A study on the applicability of proposed shear strength equation to PC beams using steel reinforcement will be reported.

Acknowledgements

The authors would like to thank Dr. Nares Pantaratorn who developed the finite element program used in this study.

References

[1] JCSE Subcommittee for Studies on Continuous Fiber, "Present State of Technology Concerning Application to the Field of Civil Engineering Structures of Concrete-Base Composite Material Using Continuous Fiber", 1992 (in Japanese)
[2] Sato, Y., Ueda, T. and Kakuta, Y., "Qualitative Evaluation of Shear Resisting Behavior of Concrete Beams Reinforced with FRP Rods by Finite Element Analysis", Concrete Library International, No.24, pp.193-209, 1994
[3] Sato, Y., Ueda, T. and Kakuta, Y., "Quantitative Evaluation of Shear Strength of Concrete Beams Reinforced with FRP Rods", Journal of Materials, Concrete Structures and Pavements, JSCE, No.484/V-22, pp.157-169, 1995 (in Japanese)
[4] Ueda, T., Pantaratorn, N. and Sato, Y. ,"Finite Element Analysis on Shear Resisting Mechanism of Concrete Beams with Shear Reinforcement", Journal of Materials, Concrete Structures and Pavements, JSCE, No.520/V-28, 1995
[5] Horibe, K., Ueda, T., "Effect of Axial Compressive Force in Shear Behavior of Reinforced Concrete Beams", Proc. of the 41th Annual Conference of the Japan Society of Civil Engineers, 5, pp.329-320, 1985
[6] Niwa, J., "Equation for Shear Strength of Reinforced Concrete Beams Based on FEM Analysis", Concrete Library International, No.4, pp.283-295, 1984
[7] Sato, Y., Ueda, T. and Kakuta, Y., "Analytical Evaluation of Shear Resisting Behavior of Prestressed Concrete Beams Reinforced with FRP Rods", Transaction of the Japan Concrete Institute, Vol.16, pp.425-430, 1994
[8] Nomura, K. and Ueda, T., "Effect of Axial Force in Strain Behavior of Stirrup", Proc. of the 40th Annual Conference of the Japan Society of Civil Engineers, 5, pp.223-224, 1984 (in Japanese)
[9] Wakui, H. and Tottori, S., " Reinforcing Effect of Spiral FRP Rods as Shear Reinforcement", Proc. of JCI, Vol.12, No.2, pp.1141-1146, 1990 (in Japanese)